J Appl Electrochem (2008) 38:1435–1443
DOI 10.1007/s10800-008-9586-3

ORIGINAL PAPER

Deposition of Zn–Cr alloy coatings from sulfate electrolyte: effect of polypropylene glycol 620 and glycine and combinations thereof

Tz. Boiadjieva · D. Kovacheva · L. Lyutov · M. Monev

Received: 4 May 2007 / Accepted: 30 April 2008 / Published online: 17 May 2008

Abstract The effect of polypropylene glycol with molecular mass 620 (PPG 620) and glycine as additives in electrodeposition of Zn–Cr alloy coatings from acidic sulfate electrolyte containing $(NH_4)_2SO_4$ and H_3BO_3, at ambient temperature, without agitation is investigated. PPG 620 inhibits the Zn reaction causing significant proximity of the deposition potentials of Zn and Cr, and a co-deposition at a less negative potential of −1.8 V (vs. Hg/Hg_2SO_4) as compared to the case when polyethylene glycol 1500 (PEG 1500) is used. Depending on the deposition conditions, alloy coatings containing up to 23 mass % Cr can be obtained. Glycine itself does not facilitate the co-deposition of Cr and Zn. Added to the electrolyte containing PPG 620, glycine causes a decrease of the Cr content in the alloy. However, the alloy coatings deposited in the presence of both additives are denser, have better overall appearance and good adherence to the steel substrate. Moreover, glycine increases the buffer capacity of the electrolyte. At short deposition times, the alloy coatings consist mainly of bcc Γ_x-(Zn, Cr) phase with lattice parameter about 3.035 (3) Å and mean crystallite size of the order of 25 nm. Cr content in the coatings can be controlled by changing the concentration of Cr(III) and pH of the electrolyte as well as the current density. Depending on the working conditions, the cathode current efficiency is within 35–55%.

Keywords Electrodeposition · Zn–Cr alloys · Polypropylene glycol · Glycine · Cyclic voltammetry · XRD

1 Introduction

Zn–Cr alloy coatings with Cr content up to 1 mass % can be deposited from electrolytes in the absence of special additives [1]. In order to achieve higher Cr content, it is necessary to include inorganic and/or organic compounds in the electrolyte. Oxygen-containing colloids [2], and compounds from the group of polyoxialkylene [3–8], phenylthiourea [9], aminoacids [10] have been suggested as such additives.

In our earlier work the effect of PEG 1500 on co-deposition of Cr and Zn from acidic electrolyte containing sulfates of Zn, Cr and Na was reported [1]. It was confirmed that addition of PEG inhibits the Zn reaction and increases the proximity of the deposition potentials of Zn and Cr [11]. Co-deposition is established at a potential of about −1.95 V (vs. Hg/Hg_2SO_4), which is achieved under galvanostatic conditions at about 20 A dm^{-2}. Depending on the deposition conditions, alloy coatings containing up to 28 at. % Cr were obtained. They are formed by local crystal growth building an island structure, which covers the surface during the deposition process. The coatings consist of two phases. During the initial stages of the

Tz. Boiadjieva
Center of Competence in Applied Electrochemistry GmbH, 2700 Wiener Neustadt, Austria

D. Kovacheva
Institute of General and Inorganic Chemistry, Bulgarian Academy of Sciences, 1113 Sofia, Bulgaria

L. Lyutov
Department of Chemistry, St. Kliment Ohridski University of Sofia, 1164 Sofia, Bulgaria

M. Monev (✉)
Institute of Physical Chemistry, Bulgarian Academy of Sciences, 1113 Sofia, Bulgaria
e-mail: monev@ipc.bas.bg

electrocrystallization the bcc Γ_x-(Zn, Cr) phase predominates. As the duration of the deposition increases, the Cr content in the Γ_x-(Zn, Cr) phase decreases and the relative content of the hcp η_x-Zn phase increases.

In search of conditions for preparation of alloys with better characteristics, the effect of other additives was also studied. It was found that improvement could be achieved when glycine (H_2N-CH_2-COOH) is added to an electrolyte containing polyoxialkylene (PEG or PPG) [12]. However, it is believed, that ammonium ions are necessary to achieve adequate interaction of Cr(III) with glycine [10, 13]. The mechanism of the effect of ammonium ions during the Zn–Cr co-deposition is not clear yet. It is assumed that their buffering action suppresses the increase in pH near the cathode [14]. According to other authors the ammonium ions do not act as a buffer, but rather as ligands, thus affecting the acidity of the aqua-chromium (III) complexes [15]. Titration curves of electrolytes based on Cr(III) show that precipitation of chromium hydroxide does not occur up to a pH of about 6. It is suggested that the ammonium ions participate in the formation of chromium complexes by substituting the bridging hydroxyl-ligands, thus suppressing the precipitation of chromium hydroxide [13]. In the presence of relatively high concentrations of ammonium ions, the substitution of ligands competes with the process of ollation [16]. Another assumption is binding of ammonium ions with the forming surface chromium hydroxide at the cathode thus facilitating its reduction [6].

From another point of view, some experimental work has been devoted to investigations on the interaction of alkaline metals from aqueous solutions with different electrodes [17, 18]. It has been established, that under cathode polarization between −1.1 and −2.2 V (NHE), it is possible to incorporate and deposit the alkaline metal within the cathode surface. A vacancy mechanism of cathode incorporation of the alkaline metals has been suggested. Investigations in electrolytes containing sulfuric acid and Zn in the presence of Na ions show a decrease in current efficiency for the Zn reaction, and an increase in current efficiency for the hydrogen reduction reaction [19]. The process of incorporation of Na and Zn ions is related to the following reactions [20]:

$$mZn + Na^+ + e^- \rightarrow NaZn_m \quad (1)$$

$$NaZn_m + H_2O \rightarrow mZn + Na^+ + OH^- + 1/2H_2 \quad (2)$$

Hydrogen, generated at the cathode surface during reaction (2) can partially penetrate into the steel substrate.

Another problem during Zn–Cr alloy deposition is the rapid pH increase in the vicinity of the cathode during the electrodeposition process. The most common buffering agent for deposition of Cr coatings based on Cr(III) is H_3BO_3, in spite of the fact that its buffering action appears at pH near 9 (pK_a about 9) [21]. Measurements of pH show an increase from 0.6 within the volume of the electrolyte to about 2.56 in the diffusion layer [13]. According to some authors, it is possible that H_3BO_3 serves as an electron bridge, thus catalyzing the reduction process, as well as widening the interval for deposition of bright coatings [22]. H_3BO_3 is also a component of weakly acidic electrolytes for deposition of Zn coatings. According to Watson et al. in electrolytes for Zn–Cr alloy deposition it plays the role of a ligand, which affects the acidity of the aqua-chromium complexes [15].

Considering the literature data, the electrolyte composition, used in previous studies, was modified by substituting Na_2SO_4 for $(NH_4)_2SO_4$ and including H_3BO_3. However, no significant change in the course of the voltammograms in the absence of additives was established. The Cr content in galvanostatically deposited coatings remains about 1 mass %.

In this work the effects of PPG 620 and glycine additives and combinations thereof on Zn–Cr co-deposition and the properties of the resulting alloy coatings are investigated using the modified electrolyte.

2 Experimental

All chemicals used were of analytical grade. Chromium sulfate was obtained by reduction of CrO_3 with ethanol in the presence of sulfuric acid. A sophisticated procedure of purification was applied and the final product crystallized in violet modification having the formula: $[Cr(H_2O)_6]_2(SO_4)_3 \cdot 6H_2O$. This crystalline product is very pure and does not contain organic impurities.

An electrolyte with the following base composition was used (g l^{-1}):

$ZnSO_4 \cdot 7H_2O$	172.5
$[Cr(H_2O)_6]_2(SO_4)_3 \cdot 6H_2O$	143.2
$(NH_4)_2SO_4$	22.0
H_3BO_3	30.0

PPG 620 and glycine were used as additives. The electrolyte compositions for the different experiments are given in Table 1.

The effect of electrochemical conditions on Zn–Cr co-deposition was investigated using cyclic voltammetry in a three-electrode cell having volume of 50 ml, reference Hg/Hg_2SO_4 electrode, working Pt electrode with surface area of 0.16 cm^2, and Pt counter electrode. The scanning rate was 25 mV s^{-1}. All experiments were carried out using a potentiostat/galvanostat model 263A (EG&G Princeton Applied Research, USA) and software SoftCorr II.

Table 1 Electrolyte composition

Component/g l^{-1}	Bath 1	Bath 2	Bath 3	Bath 4	Bath 5	Bath 6
$ZnSO_4 \cdot 7H_2O$	172.5	172.5	172.5	172.5	172.5	172.5
$[Cr(H_2O)_6]_2(SO_4)_3 \cdot 6H_2O$	–	–	143.2	143.2	143.2	143.2
$(NH_4)_2SO_4$	22	22	22	22	22	22
H_3BO_3	30	30	30	30	30	30
PPG 620	–	0.5/1.0	–	1.0	–	1.0
Glycine	–	–	–	–	45	37.5

Zn–Cr alloy coatings were deposited under galvanostatic conditions onto steel substrates with dimensions 20 × 10 mm. Pretreatment of the electrodes included electrochemical degreasing and pickling in 10% solution of H_2SO_4. Coatings were deposited at current density within the 2.5–50 A dm^{-2} interval, at pH 1.0–2.2, at 25 °C, without agitation. Platinized Ti was used as an anode.

The Cr content in the alloy coatings was determined using X-ray microprobe analysis (EDX) (JCXA 733 Jeol, Japan). The distribution of Cr into the depth of the coating was measured by glow discharge emission spectroscopy (GDOES). The cathode current efficiency was determined gravimetrically and based on data of EDX analyses. The morphology of the alloy coatings was studied using scanning electron microscopy (SEM) (JSM 5300, Jeol, Japan). Values for alloy coating thickness were obtained from X-ray fluorescence analysis (RFA).

Phase compositions of the coatings were determined using X-ray diffraction (XRD). X-ray diffraction patterns of the alloy deposits were recorded with an DRON type automatic powder diffractometer using Bragg-Brentano geometry, CuK_α filtered radiation and scintillation counter.

Surface roughness of the coatings was measured using a profilometer DEKTAK 3 Surface profile measuring system (Veeco Instruments Inc.). Surface profiles were obtained by dragging a needle to scan surface fragments of 3,000 μm for 15 s time periods.

3 Results

3.1 Effect of additives on Zn–Cr co-deposition

3.1.1 Effect of PPG 620 on Zn deposition

The strongest effect of PPG 620 is observed at a concentration of 1 g l^{-1} (Fig. 1). Increase of PPG concentration does not lead to increase in polarization. In the absence of PPG 620, the equilibrium potential of the Zn reaction is −1.43 V. The curve profile up to the latter potential is determined by the hydrogen reduction reaction and by the underpotential deposition of Zn [23]. In the presence of PPG 620 the evolution of the voltammogram is retained up to the cathode maximum at −1.34 V. The equilibrium potential is not affected, but massive Zn deposition starts at a potential of about −1.9 V, i.e. the polarization reaches 500 mV. In a manner similar to that of PEG, PPG 620 obviously slows down the growth of the Zn coating. Adsorption of PPG 620 blocks sites active for Zn ion reduction, thus hindering the surface diffusion and acting as a barrier to the transport of protons and Zn ions towards the electrode surface [24]. On the other hand, oxygen atoms in the PPG 620 molecule may act as electron-pair donors to Zn^{2+} and are likely to form complexes with the Zn ions.

3.1.2 Effect of PPG 620 on Zn–Cr co-deposition

In the presence of Cr(III), PPG 620 polarizes the overall cathode reaction by about 350 mV (Fig. 2). The maximum in the region of active dissolution of Zn and Cr has significantly smaller area. PPG 620 does not only inhibit the cathode process, but reduces the current efficiency (from 63 to 50% at 30 A dm^{-2}, 90 s, pH 1.6). A clear maximum is observed in the region of transpassive dissolution of Cr. As evident from the XRD patterns, the alloy coatings are composed of two phases. Considering their anodic behaviour in 1 M Na_2SO_4 solution, pH 5.4, the dissolution passes

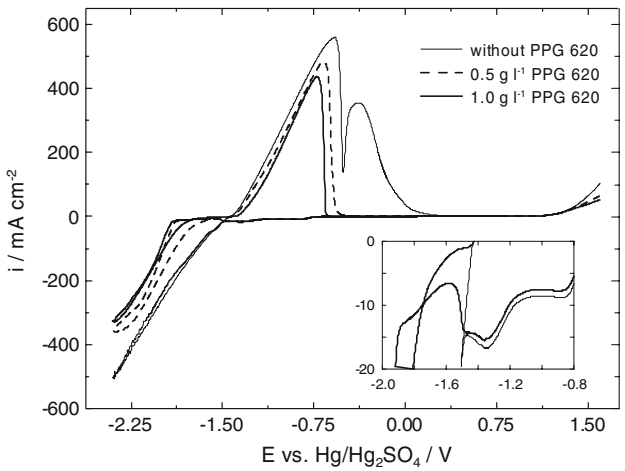

Fig. 1 Effect of the concentration of PPG 620 on the evolution of the voltammogram in Zn electrolyte. Baths 1 and 2

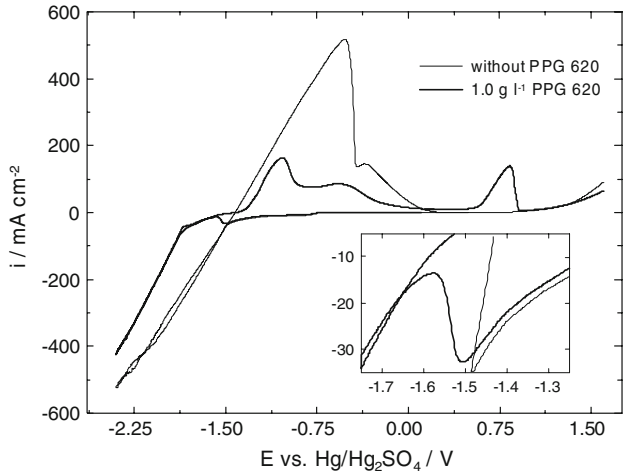

Fig. 2 Effect of PPG 620 on the voltammogram obtained in the modified electrolyte for Zn–Cr deposition. Baths 3 and 4

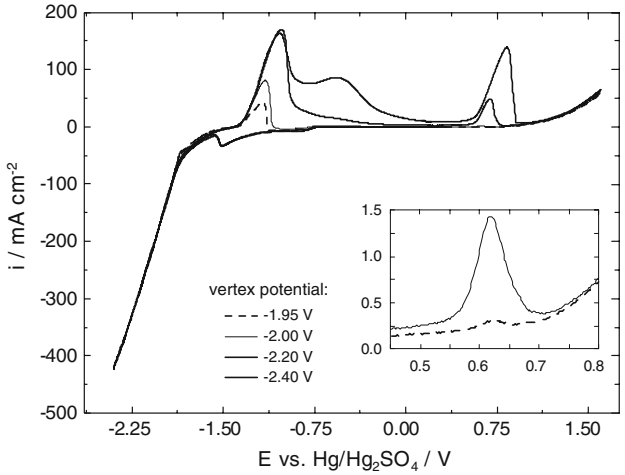

Fig. 3 Effect of the cathode potential on the deposition and dissolution of Zn–Cr in presence of PPG 620. Bath 4

through dissolution of hcp η_x-Zn phase in the region of active dissolution of Zn and Cr, selective dissolution of Zn from bcc Γ_x-(Zn, Cr) phase, and dissolution of Zn and Cr from the Γ_x-(Zn, Cr) phase at a potential close to that of transpassive dissolution of Cr [25]. A thin layer of a Γ_x-(Zn, Cr) phase rich in Cr remains on the Pt electrode. It is destroyed after the potential of oxygen evolution is reached. In the present study, when electrolyte with pH 1.6 is used, dissolution of Cr from the Γ_x-(Zn, Cr) phase in the region of active dissolution is also expected. When stirring the electrolyte during the dissolution process, the peak after the first anodic maximum disappears, this implies that it may be related not only to the phase composition, but also to diffusion limitations during dissolution.

The anodic maximum in the region of transpassive dissolution of Cr is registered upon scanning to −1.95 V vertex potential (Fig. 3). Under the galvanostatic conditions this potential is reached at about 15 A dm^{-2} (Fig. 4). At low current densities a stepwise change in potential with time is observed. The steps are more pronounced at 2.5 A dm^{-2} and correspond to the characteristic potentials determined at this current density from the voltammogram in Fig. 2. Similar steps are also observed on cathodic polarization in zinc electrolyte. At about −1.3 V, evolution of hydrogen alone should be expected. However, the underpotential deposition of Zn impedes the hydrogen reduction reaction and the potential shifts towards the region of Zn bulk deposition [23].

Coatings deposited in the presence of PPG 620 are grey. The observations by SEM did not show significant differences in the morphology of the coatings as a function of current density. The morphology displays agglomeration of crystallites and a non-compact structure (Fig. 5). According to the XRD studies the crystallite size is of the order of 50 nm.

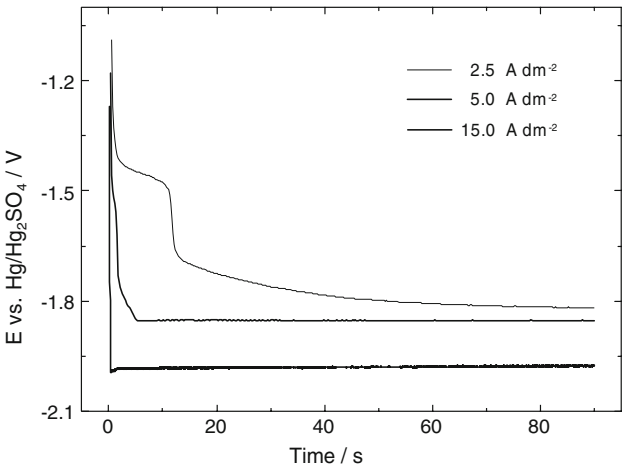

Fig. 4 Potential vs. time curves at different current densities. Bath 4

3.1.3 Effect of glycine on co-deposition of Cr and Zn

Addition of glycine leads to deposition of shiny and dense Cr coatings [26]. Therefore glycine is used also for deposition of Cr-Ni coatings from sulfate electrolytes [27]. Glycine was one of the first complexation agents suggested for production of Cr coatings from electrolytes based on Cr(III) [28]. Besides complexation, significant surfactant action of glycine is established. At low concentrations insufficient for complexation of the Cr(III) the current efficiency with respect to Cr decreases significantly. Investigations show that high quality Cr coatings can be obtained at high deposition rates using a glycine to Cr(III) molar ratio of 1:1. Glycine is also used for deposition of Zn–Cr alloy coatings [10, 13]. Both these papers imply formation of a number of complexes with different extent of protonation of the glycine.

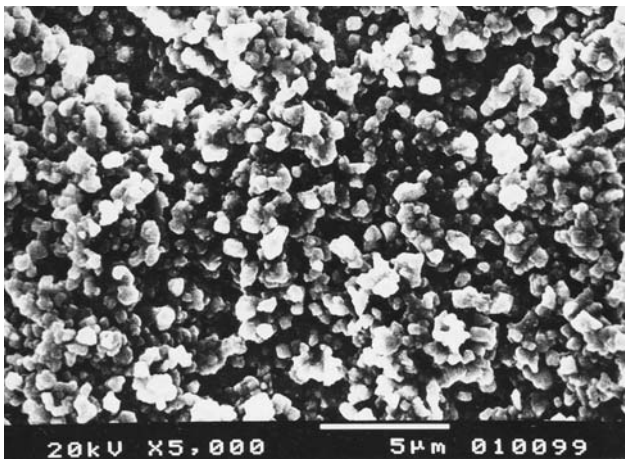

Fig. 5 Morphology of the Zn–(21 mass %)Cr alloy coating deposited from bath 4 at pH 1.6 and 30 A dm^{-2} for 90 s

In the present investigations glycine was added to the electrolyte at concentrations up to 0.6 mol l^{-1} (Bath 5). X-ray microprobe analysis of the samples deposited under galvanostatic conditions at pH 1.0 and 1.6 shows that the coatings do not contain Cr.

3.1.4 Effect of combination of additives on co-deposition of Cr and Zn

Addition of glycine to electrolyte containing PPG 620 reduces the bi-component anodic maximum in the region of active dissolution of Zn and Cr to a single peak (Fig. 6). A similar effect was observed when coatings with high Cr content were dissolved in the electrolyte containing 0.5 M $(NH_4)_2SO_4$. It is possible that glycine and $(NH_4)_2SO_4$ affect the formation of the barrier film in the region of active dissolution by forming complexes with ions from the dissolving coating and thus facilitate the dissolution process. At this electrolyte pH stronger complexation between glycine and Cr ions (than glycine-Zn ions) is expected [29], leading to complete dissolution of the residual Γ_x-(Zn, Cr) phase in the transpassive region; thus the anode maximum is better pronounced. The shape of the voltammogram is apparently related to the alloy composition. As shown by further investigation, in the presence of glycine, the Cr content in the coatings decreases significantly.

A series of voltammograms to different vertex cathode potentials shows an anodic maximum within the region of active dissolution of Zn and Cr after scanning to −1.6 V (Fig. 7a). After dissolution of reduced Zn species, the curve goes into the cathode region as the Pt electrode remains in the region of hydrogen evolution. Upon scanning to −1.9 V, the maximum in the active dissolution region is split (Fig. 7a) and that in the region of transpassive dissolution of Cr is clearly pronounced (Fig. 7b). Comparison with a voltammogram in a Cr electrolyte

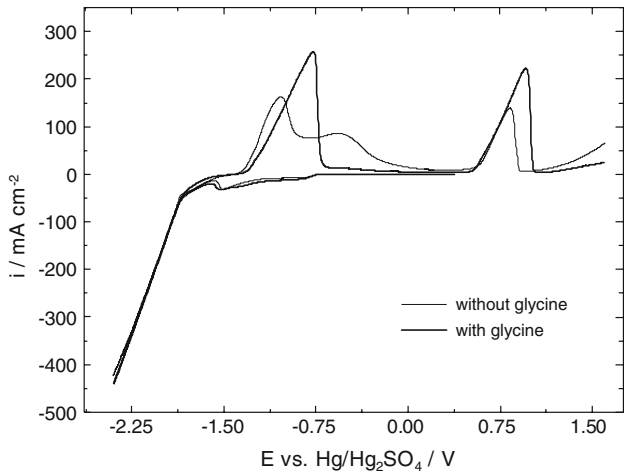

Fig. 6 Voltammograms showing the effect of glycine on the deposition and dissolution of Zn–Cr in electrolyte containing PPG 620. Baths 4 and 6

shows that the splitting is due to active dissolution of Cr. Scanning to more negative potentials causes a significant increase in both anodic maxima and a shift of the maxima towards more positive potentials (Fig. 7b).

Glycine added to electrolyte containing PPG 620 does not change the potential of massive co-deposition of Cr and Zn. Potentiodynamic curves of the dissolution of alloy layers deposited under different current densities (Fig. 8) show that Cr is co-deposited with Zn at a current density of about 2 A dm^{-2} (Fig. 9), i.e. the co-deposition potential is reached at lower current density as compared to that for the electrolyte containing no glycine. However, higher than 2 A dm^{-2} is needed to obtain "real" alloy coatings. Upon increasing the current density to 15 A dm^{-2} the areas of the anodic maxima increase (Fig. 9). Current densities higher than 30 A dm^{-2} do not cause significant change in the evolution of the dissolution curves, i.e. higher polarization does not cause an increase in Cr content in the alloy. In support of these investigations the data in Table 2 imply that, within the interval 20–50 A dm^{-2}, Cr content depends only slightly on current density. Most likely this is due to a pH increase near the electrode surface, transformation of the Cr(III) complexes and reduction of the amount of electroactive Cr(III) species.

Figure 10 shows that addition of glycine yields denser and smoother coatings.

3.2 Effect of working conditions on co-deposition of Cr and Zn

Upon decreasing the pH from 1.6 to 1.0 the rate of the overall cathode reaction increases (Fig. 11). The areas under the anodic maxima in the region of active dissolution for Zn and Cr are similar, but those in the range of transpassive dissolution of Cr decrease. Results from X-ray

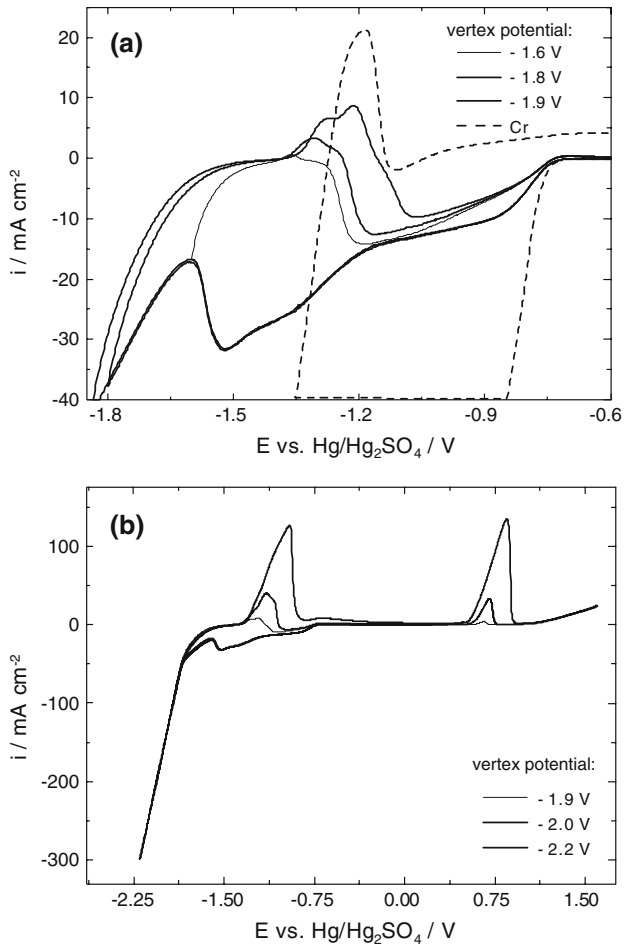

Fig. 7 Voltammograms showing the effect of cathode potential on deposition and dissolution of Zn–Cr in presence of PPG 620 and glycine: (**a**) vertex potentials to −1.9 V; (**b**) vertex potentials to −2.2 V. Bath 6

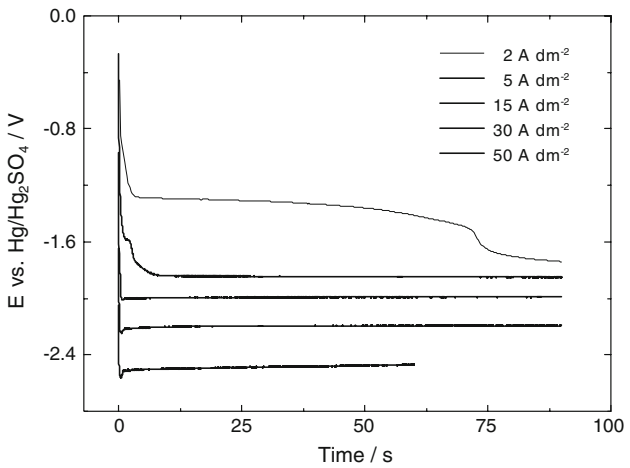

Fig. 8 Galvanostatic potential vs. time curves obtained during Zn–Cr deposition at different current densities. Bath 6

microanalysis of coatings deposited from the same electrolyte at different pH are presented in Table 2. Increasing pH up to 2.0 yields coatings with higher Cr content. Further

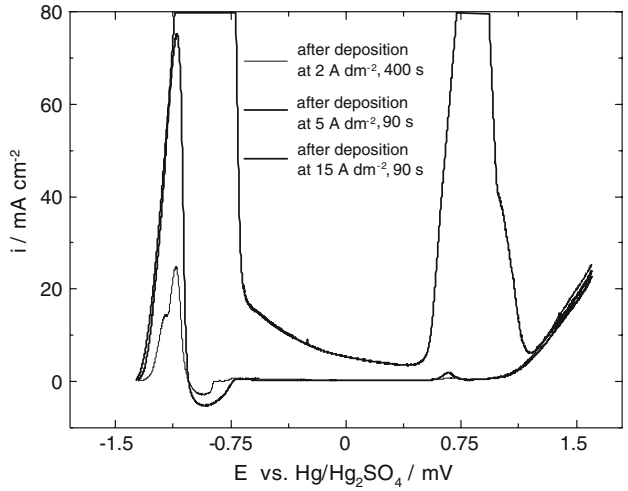

Fig. 9 Potentiodynamic curves of dissolution of Zn–Cr alloy coatings deposited at 2, 5 and 15 A dm^{-2}. Bath 6

increase in pH reduces the Cr content and the coatings become darker.

Cr content in the coatings can also be varied by changing the Cr(III) concentration in the electrolyte (Table 3). It can be seen that the presence of glycine causes a decrease in Cr content in the alloy.

3.3 Properties of electrolyte and alloy coatings

3.3.1 Cathode current efficiency

In contrast to data obtained for the effect of glycine on the deposition of Cr coatings [26], no decrease in current efficiency is found during alloy deposition in this study. One likely reason is the weak dependence of the mass of deposited Zn on the presence of glycine. Upon decrease in pH and increase in current density, the cathode current efficiency for the alloy decreases. Depending on the working conditions the values fall in the range 35–55%.

3.3.2 Electrolyte buffer capacity

Very good buffering action of glycine is found in sulfate electrolytes for deposition of Cr coatings [26]. The present investigations also show a higher buffer capacity of the electrolyte for deposition of Zn–Cr alloy coatings when it contains glycine (Fig. 12).

3.3.3 Morphology and composition of Zn–Cr alloy coatings

SEM images of samples at different stages of the deposition process are shown in Fig. 13. During the initial stages of growth, an island structure similar to that obtained from the electrolyte containing Na_2SO_4 is observed [1]. The

Table 2 Dependence of Cr content in Zn–Cr alloy coatings on deposition conditions. Bath 6

Current density/A dm^{-2} (pH 1.6, 90 s)	Cr mass %	pH (30 A dm^{-2}, 90 s)	Cr mass %	Deposition time/s (pH 1.6, 30 A dm^{-2})	Cr mass %
2.5	0	1.0	5.5	10	21.4
15	4.1	1.3	11.0	30	14.9
20	14.0	1.6	14.0	90	14.0
30	14.0	2.0	18.0	300	7.2
50	14.8	2.2	12.5	600	0.5

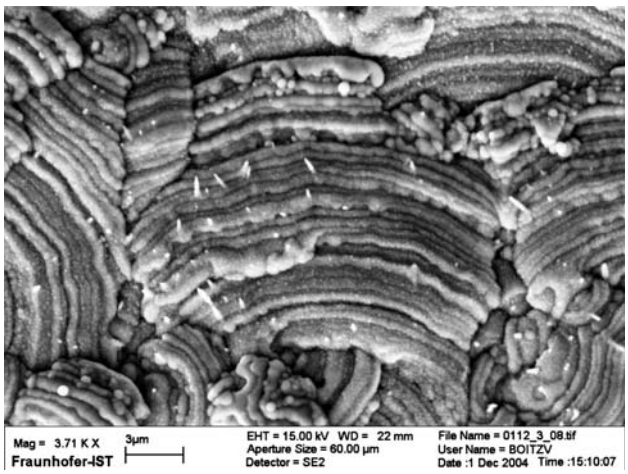

Fig. 10 Morphology of Zn–Cr alloy coating deposited at pH 1.6, 30 A dm^{-2} for the duration of 90 s. Bath 6

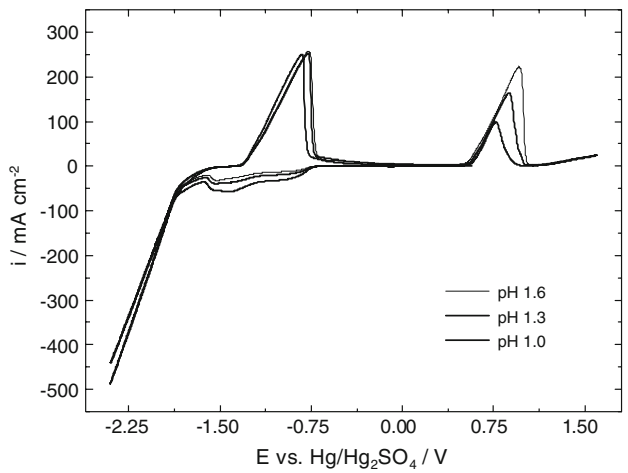

Fig. 11 Voltammograms showing the effect of the electrolyte pH on the deposition and dissolution of Zn–Cr. Bath 6

Table 3 Effect of Cr(III) concentration in the electrolyte on Cr content in the Zn–Cr alloy coatings. pH 1.6, c.d. 30 A dm^{-2}, 90 s

Cr(III)/mol l^{-1}	Basic electrolyte + PPG 620 (Bath 4)	Basic electrolyte + PPG 620 + glycine (Bath 6)
0.2	8	8
0.4	21	14
0.8	27	19

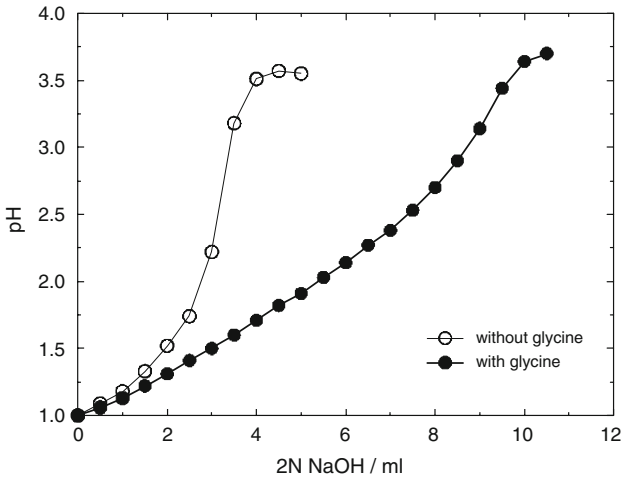

Fig. 12 Titration curves of electrolyte with and without glycine. Baths 4 and 6

formations have various sizes—from nano- to micrometers and a Cr content of 21–23 mass %. Increased deposition times result in filling up the surface, increased thickness of the coatings and a drastic decrease in average Cr content (Table 2). A gradient in the distribution of Cr into the depth of the coating is observed, as near the surface the Cr content decreases significantly (Fig. 14).

From the electrolyte without additive coatings consisting of hcp η_x-Zn phase with unit cell parameters a = 2.66 (1) Å and c = 4.97 (1) Å are deposited (Fig. 15a). In the coatings deposited in the presence of PPG 620 (Fig. 15b), as well as in presence of the combination of PPG 620 and glycine (Fig. 15c), the bcc Γ_x-(Zn, Cr) phase predominates with lattice parameters 3.033 (3) Å and 3.035 (3) Å. Thus addition of glycine does not significantly change the content of Cr in the Γ_x-(Zn, Cr) phase. However, the mean size of the crystallites of the Γ_x-(Zn, Cr) phase decreases from 50 to 25 nm and the relative contribution of the η_x-Zn phase increases.

3.3.4 *Roughness*

Addition of glycine to the electrolyte containing PPG 620 causes significant smoothing of the surface. Samples deposited in the presence of glycine display an average roughness of 1 µm, which is one and a half times lower

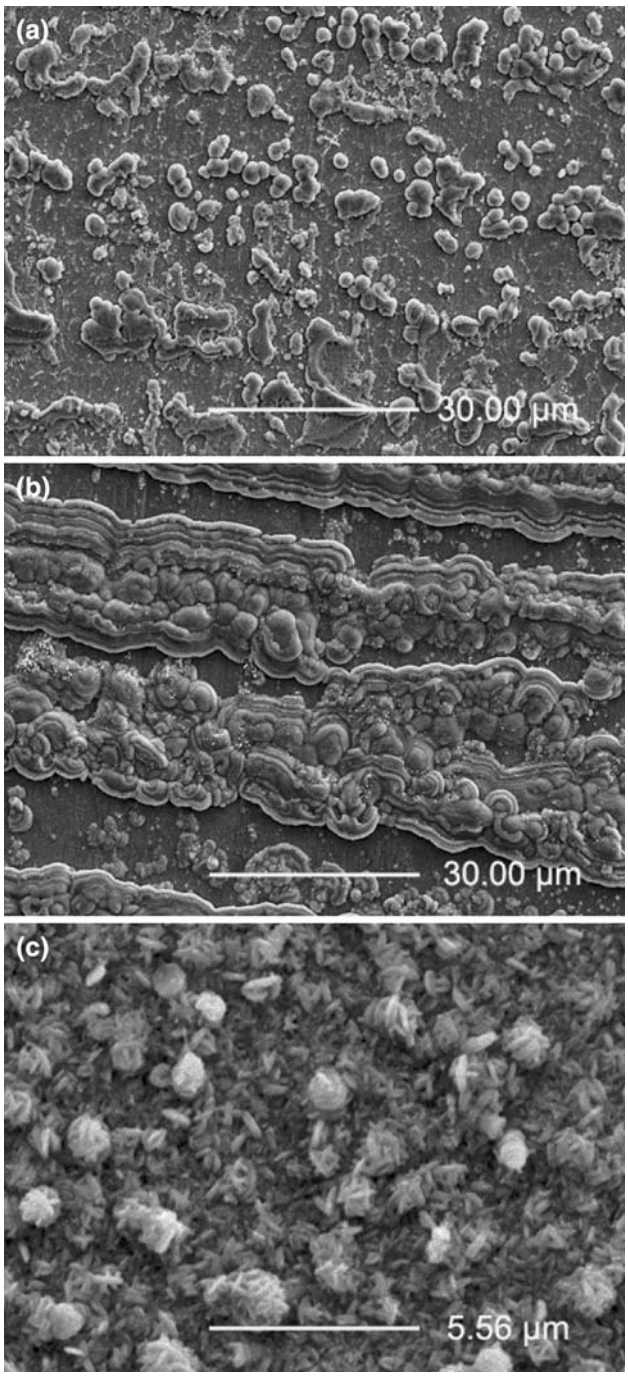

Fig. 13 Effect of deposition time on the morphology of Zn–Cr coatings obtained in presence of PPG 620 and glycine at 30 A dm^{-2}: (**a**) 5 s, (**b**) 30 s, (**c**) 600 s. Bath 6

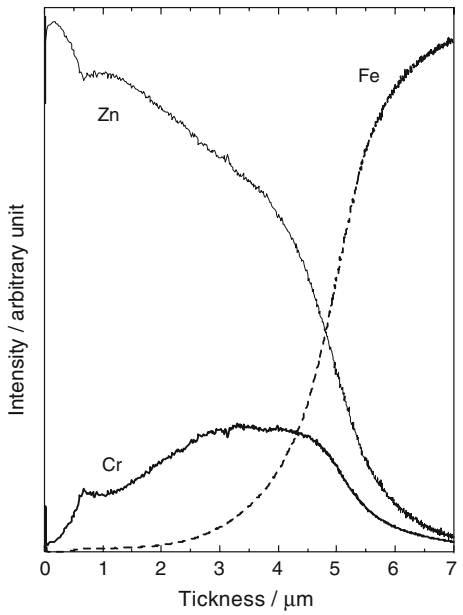

Fig. 14 GDOES profile of Zn-14 mass % Cr alloy coating

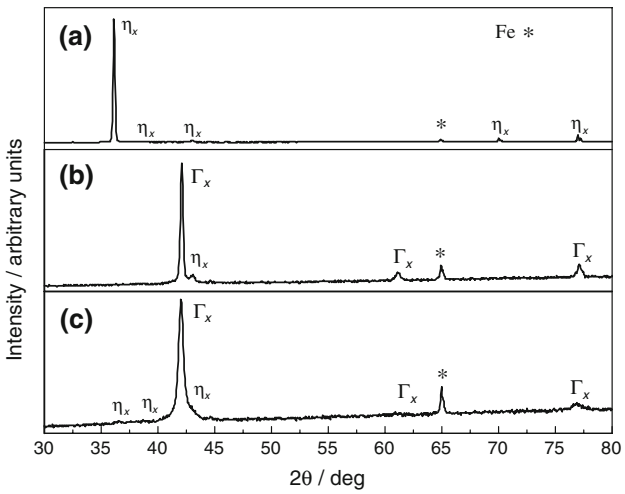

Fig. 15 XRD spectra of Zn–Cr alloy coatings following deposition from different electrolytes: (**a**) without additives (Bath 1), (**b**) containing PPG 620 (Bath 4), (**c**) containing PPG 620 and glycine (Bath 6). pH 1.6, 30 A dm^{-2}

than that of samples deposited from basic electrolyte containing only PPG 620 additive.

4 Conclusions

PPG 620 facilitates the co-deposition of Cr and Zn mainly by inhibiting the Zn deposition reaction. As a result, significant proximity of the deposition potentials of Zn and Cr is achieved as well as co-deposition at less negative potential −1.8 V as compared to the case when PEG 1500 or PEG 6000 are used. Alloy coatings containing up to 23 mass % Cr can be deposited.

Glycine itself does not facilitate co-deposition of Cr and Zn and, when added to an electrolyte containing PPG 620, causes a decrease in Cr content in the coatings. Electrolyte containing glycine has higher buffer capacity, which makes deposition of alloy coatings possible at relatively high pH values (about pH 2 in the bulk of the electrolyte).

In coatings deposited in the presence of PPG 620, as well as in the presence of a combination of PPG 620 and glycine the Γ_x-(Zn, Cr) phase predominates. The addition of glycine does not significantly change the Cr content in the Γ_x-(Zn, Cr) phase, but the size of the crystallites with Γ_x-(Zn, Cr)-type phase decreases from 50 to 25 nm and the relative contribution of the η_x-Zn phase increases.

The Cr content in the coatings can be varied by changing current density, pH, Cr(III) concentration and deposition time. Depending on the working conditions the cathode current efficiency lies between 35 and 55%.

Alloy coatings deposited in the presence of both additives are denser, have better appearance, better adherence to the steel substrate and, despite the lower average Cr content, their corrosion-electrochemical behavior is improved as compared to coatings deposited in the presence of PPG 620 alone [25].

References

1. Boiadjieva Tz, Kovacheva D, Petrov K, Hardcastle S, Sklyarov A, Monev M (2004) J Appl Electrochem 34:315
2. Takahashi A, Miyoshi Y, Hada T (1994) J Electrochem Soc 141:954
3. US Patent 4 877 494, EP 0 285 931 A1
4. US Patent 4 897 317
5. US Patent 5 510 196, EP 0 607 452 A1, EP 0 607 452 B1
6. EP 0 638 668 A1
7. EP 0 643 157 A1
8. Ohgai T, Ki J, Akiyama T, Fukushima H (1998) In: Cho WD, Sohn HY (eds) Value-addition metallurgy, University of Utah, Salt Lake City, Utah, pp 225
9. US Patent 5 618 634
10. Berezin N, Gudin N, Filippova A, Matulenis E, Borisov Yu (1993) Zashchita Metallov 29:99
11. Akiyama T, Kobayashi S, Ki J, Ohgai T, Fukushima H (2000) J Appl Electrochem 30:817
12. Boiadjieva Tz, Monev M, Raichevski G (2004) IV Intern Cong "Mechanical Engineering'04", September, Varna, vol 5/7311, pp 246
13. El-Sharif M, McDougall J, Chisholm C (1999) Trans Inst Met Fin 77:139
14. El-Sharif M, Chisholm C, Sut Y, Feng L (1997) Roy Soc Chem (Adv Surf Eng 1) 206:95
15. Watson A, Su YJ, el-Sharif MR, Chisholm CU (1993) Trans Inst Met Fin 71:15
16. Rollinson CL (1973) The chemistry of Chromium, Molybdenum and Tungsten. Pergamon Press, Oxford, New York, Toronto, Sydney, Paris, Braunschweig
17. Kabanov B, Leikis D, Kisileva I, Astahov I, Aleksandrova D (1962) Dokl Akademii nauk SSSR 144:1085
18. Kabanov B, Astahov I, Kisileva I (1965) Uspehi himii 34:1813
19. Turomshina U, Stender B (1955) J prikl himii 28:166
20. Bagaev SP, Kudrjavzev WN, Pedan KS (1983) Elektrochimija 19:509
21. Pearson T, Long E (1998) Trans Inst Met Fin 76:B 83
22. Falicheva A, Spiridonov B (2001) J prikl himii 74:1784
23. Boiadjieva Tz, Monev M, Tomandl A, Kronberger H, Fafilek G (2008) submitted for publication
24. Lee JY, Kim JW, Lee MK, Shin HJ, Kim HT, Park SM (2004) J Electrochem Soc 151:C25
25. Boiadjieva Tz, Petrov K, Raichevski G, Monev M (2006) Trans Inst Met Fin 84:313
26. Lausmann G, Unruh J (1998) Die galvanische Verchromung. Eugen G. Leuze Verlag, Saulgau/Württ
27. Elektroosajdenie metallov I splavov (1966) In: Itogi nauki, Elektrohimija, Vijpusk I, Moskva
28. Radjuvene B, Skominas Yu (1986) Trudi Akademii nauk Litovskoj SSSR Serie Ь 4:25
29. Ortiz-Aparicio JL, Meas Z, Trejo G, Ortega R, Chapman TW, Chainet E, Ozil P, (2007) Electrochim Acta 52:4742